

Forcing aggregation of cyanine dyes with salts: A fine line between dimers and higher-ordered aggregates

Sara M Mooi, Samantha N. Keller and Belinda Heyne*

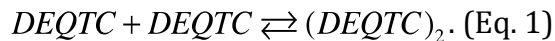
Chemistry Department, University of Calgary, 2500 University Drive N.W. Calgary, Alberta, T2N 1N4, Canada

Email: bjmheyne@ucalgary.ca

1.	Variable temperature study performed to demonstrate a monomer-dimer equilibrium of DEQTC in aqueous solution.	S2
2.	Evaluation of the equilibrium constant using a chemometric approach and determination molar extinction coefficients for DEQTC monomeric and dimeric species.	S4
3.	Assessment of the monomeric nature for 3,3-diethylthiacyanine iodide (THIA) and 1,1'-diethyl-2,2'-cyanine iodide (PIC).	S10
4.	Chemometric approach in order to evaluate the equilibrium constant of THIA in aqueous solution.	S13
5.	DFT calculation of the various cyanine dyes employed in this study.	S15
6.	Evaluation of the DEQTC percent monomer composition before and after the addition of sodium acetate (NaCH_3CO_2), sodium chloride (NaCl), or sodium bromide (NaBr).	S19
7.	Quantification of the equilibrium constant for DEQTC upon the addition of NaCH_3CO_2 , NaCl , and NaBr .	S21
8.	Absorption spectra of THIA before and after the addition of NaCH_3CO_2 , NaCl , or NaBr .	S22
9.	Absorption of PIC before and after the addition of NaBr .	S23
10.	Absorption spectra recorded for the addition of NaI and NaBF_4 to a solution of DEQTC, THIA and PIC.	S24
11.	DFT Calculation for the ion pairs	S27

1. Variable temperature study performed to demonstrate a monomer-dimer equilibrium of DEQTC in aqueous solution.

The monomer-dimer equilibrium of 1,3'-diethyl-4,2'-quinolylthiacyanine (DEQTC) can be simply represented below, where DEQTC and $(DEQTC)_2$ represent the monomeric and dimeric forms respectively;



The equilibrium constant (K_{eq}) describing this reaction can be written as follows;

$$K_{eq} = \frac{[(DEQTC)_2]}{[(DEQTC)]^2}. \text{ (Eq. 2)}$$

Activity coefficients are not included in the equation for the equilibrium constant as they can be approximated to one at the concentrations studied.¹ The equilibrium constant for any reaction at equilibrium, including a monomer-dimer equilibrium, is related to temperature in the form of the van't Hoff equation where at a given temperature:

$$\ln K_{eq} = -\frac{\Delta G}{RT}. \text{ (Eq. 3)}$$

Consequently, a change in temperature will result in a change in the equilibrium constant and is commonly represented as follows²:

$$\ln\left(\frac{K_2}{K_1}\right) = -\frac{\Delta H^\circ}{R}\left(\frac{1}{T_2} - \frac{1}{T_1}\right). \text{ (Eq. 4)}$$

Therefore, as described by the van't Hoff equation, a change in the environment temperature of a solution will result in a change in the equilibrium of the monomer and dimer. In result, a change in the monomer and dimer intensity peaks can be monitored with UV-Vis spectroscopy for DEQTC as the monomer and the dimer forms have characteristic absorption maxima at 501 and 477 nm respectively.

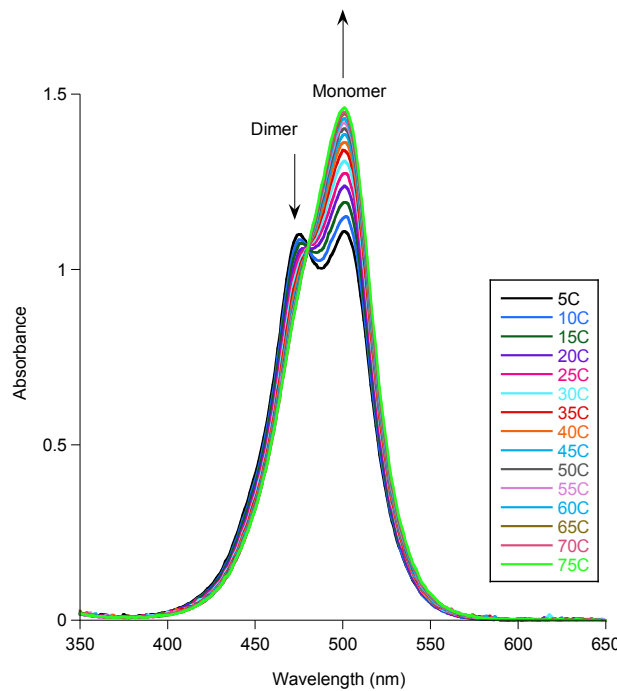


Figure S1: Absorption spectrum of a 20 μM aqueous solution of DEQTC recorded between 5°C and 75°C. The absorption spectra have been corrected for thermal expansion of water. Arrows demonstrate the movement of the absorption spectra when the temperature is increased, highlighting the change in the absorption intensities of the monomer and dimer as the temperature increased.

2. Evaluation of the equilibrium constant using a chemometric approach and determination molar extinction coefficients for DEQTC monomeric and dimeric species.

Using the software Datan (v5.0, multid) developed by Kubista,^{3, 4, 5, 6, 7, 8} the absorption spectra recorded for DEQTC 20 μ M at temperature ranging from 5°C to 75°C (278.15K - 348.15K) and corrected for thermal expansion (see below) of the solvent were analyzed simultaneously. Briefly, the software stores all the absorption spectra in a file as a matrix **A** of dimensions $n \times m$, where n represents the wavelengths and m the temperatures.^{5, 6} Using a non-linear iterative partial least square (NIPALS) algorithm, the matrix **A** of rank r is decomposed into r matrices of rank 1, which corresponds to the outer product of two vectors, the score vector, t , and the loading vector, p :

$$A = \sum_{j=1}^r t_j \otimes p_j = \sum_{j=1}^r t_j p_j^T \quad (\text{Eq. 5})$$

where the score vector t_j is a $n \times 1$ column vector, the loading vector p_j is a $m \times 1$ column vector, and T is the transpose function making thus p_j^T a $1 \times m$ row vector.^{5, 6} The rank of the matrix **A**, r , corresponds to the number of independent absorbing species accounting for in the absorption spectra.^{5, 6} It is important to note that the vectors t_j and p_j do not correspond to any component of the spectra, as they are simple mathematical constructs.^{5, 6} These vectors are not calculated all at once but rather pair-by-pair, via an iterative method. Goodness of the solution is ensured when a minimum value of a χ^2 statistical analysis is reached. The method is explained in more details in several publications.^{3, 4, 5, 6, 7, 8}

The figures bellow present the results obtained from the chemometric analysis of a 20 μM aqueous solution of DEQTC in term of a Van't Hoff plot expressing the variation of K_{eq} in function of temperature. The software allows also for the absorption spectra for the monomeric and dimeric species of DEQTC to be calculated. The same experiment and analysis was performed using a 20 μM aqueous solution of TO^+ for comparison.

Absorption spectra were carried out in a 1 cm x 1 cm plastic cuvette in order to minimize adsorption of the cyanine dyes on the cuvette's walls. Measurements were performed on a Varian Cary-50 single beam spectrophotometer at temperature ranging from 278.15K to 348.15K, by 5K increments. Absorption spectra were corrected for thermal expansion of water, according to the following expression:

$$A_{\text{corr}} = \frac{A(T_f)_{\text{meas}} V_i(T_i) (1 + \alpha(T_i)(T_f - T_i))}{V_{\text{desired}}}, \text{ (Eq. 6)}$$

where A_{cor} represents the corrected absorption spectrum, A_{meas} is the measured absorption spectrum, T_i and T_f are the initial and final temperature in Kelvin, V_i is the initial volume, V_{desired} is the volume of the solution prepared at room temperature, which is 3 mL in our case, and α is the thermal expansivity of water.⁹

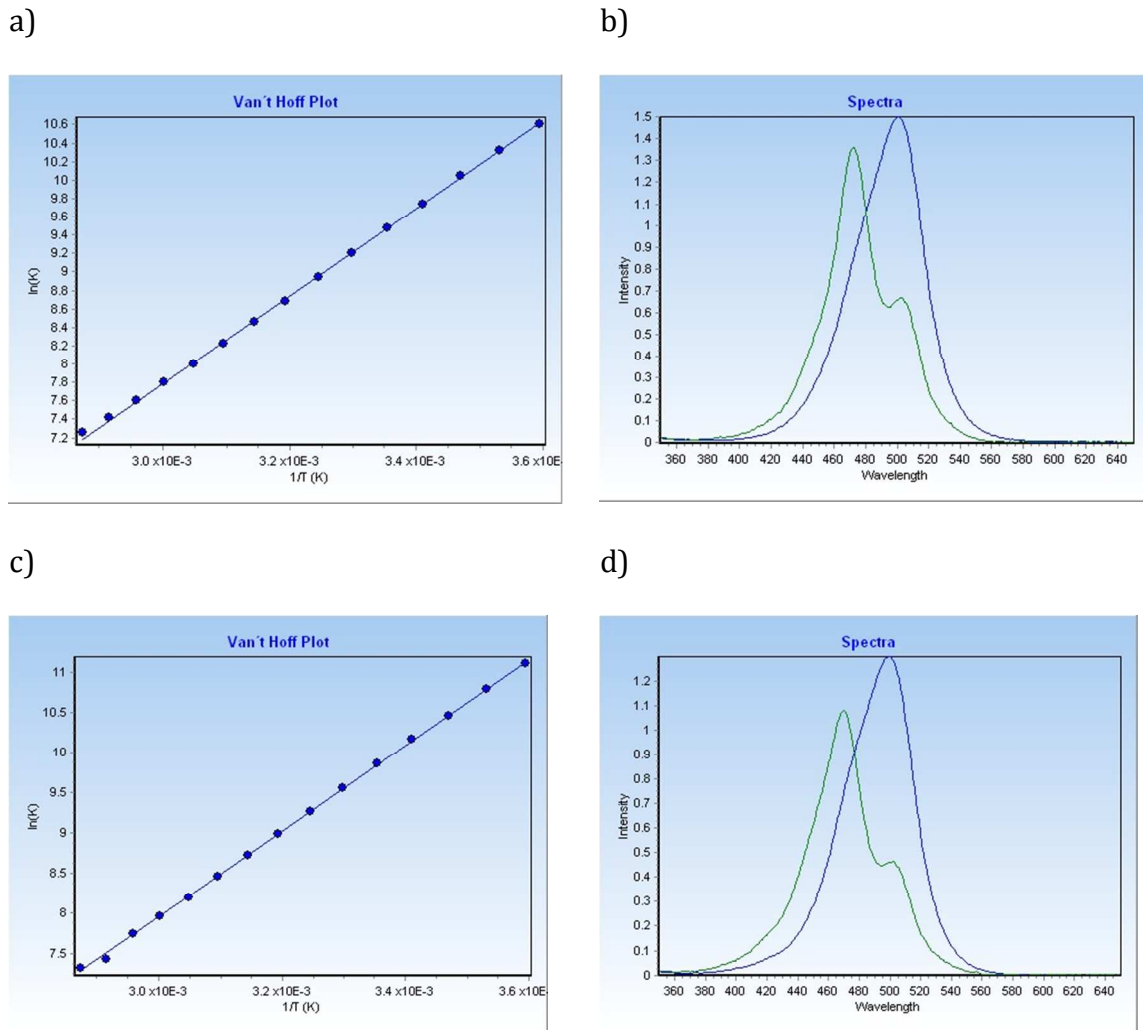


Figure S2: a) and c) Van't Hoff plot in 5K interval between 278.15K and 348.15K; b) and d) calculated absorption spectra for the monomer (blue) and dimer (green) of DEQTC (20 μ M, a and b) and TO⁺ (20 μ M, c and d) in water.

The equilibrium constants K_{eq} for both DEQTC and TO⁺ are reported in table S1 below. According to our data, DEQTC presents a smaller K_{eq} than the one measured for TO⁺, suggesting DEQTC is less inclined at forming dimers in aqueous solution. Moreover, the DATAN software provides an average standard enthalpy change (ΔH^0) and standard entropy change (ΔS^0) of -39.5 kJmol⁻¹ and -53.8 JmolK⁻¹, respectively, for DEQTC and -44.2 kJmol⁻¹ and -66.3 JmolK⁻¹ for TO⁺. These results

indicate that aggregation of both dyes is enthalpy favored and entropy disfavored, which was expected. The smaller enthalpy change reported for DEQTC compared to TO^+ suggests a more hindered association of this cyanine dye in aqueous solution, which can be understood in term of the steric hindrance brought by the ethyl groups present on DEQTC.

As mentioned previously, the monomeric and dimeric forms of DEQTC are in equilibrium at room temperature. Equation 1 describes this equilibrium and thus Equation 2 can represent the equilibrium constant. At any concentration of DEQTC, a conservation of mass equation can be written where the total concentration of DEQTC (C_T) is described in forms of its equilibrium monomer and dimer concentrations;

$$C_T = [\text{DEQTC}] + 2[(\text{DEQTC})_2]. \text{ (Eq. 7)}$$

At any concentration of DEQTC, the absorption intensity at a given wavelength (A^λ) is a function of the concentrations of the monomer and dimer along with their extinction coefficients at the given wavelength, ε_m^λ and ε_d^λ respectively, and can be expressed as follows:

$$A^\lambda = (\varepsilon_m^\lambda [\text{DEQTC}] + \varepsilon_d^\lambda [(\text{DEQTC})_2])l. \text{ (Eq. 8)}$$

A^λ can be written in terms of the total concentration of DEQTC and the equilibrium constant by incorporating Equations 3, 4, and 7 into Equation 8;

$$A^\lambda = \left\{ \left(\varepsilon_m^\lambda - \frac{\varepsilon_d^\lambda}{2} \right) \left(\frac{-1 + \sqrt{1 + 8K_{eq} C_T}}{4K_{eq}} \right) + \frac{\varepsilon_d^\lambda}{2} C_T \right\} l. \quad (\text{Eq. 9})$$

Knowing the equilibrium constant at 20°C (Figure S2), the extinction coefficients for DEQTC monomer and dimer were extrapolated from a linear regression analysis using Equation 9 (Figure S3). The extinction coefficients for the monomer and dimer both at 477 and 501 nm, along with the equilibrium constant are summarized in Table S1.

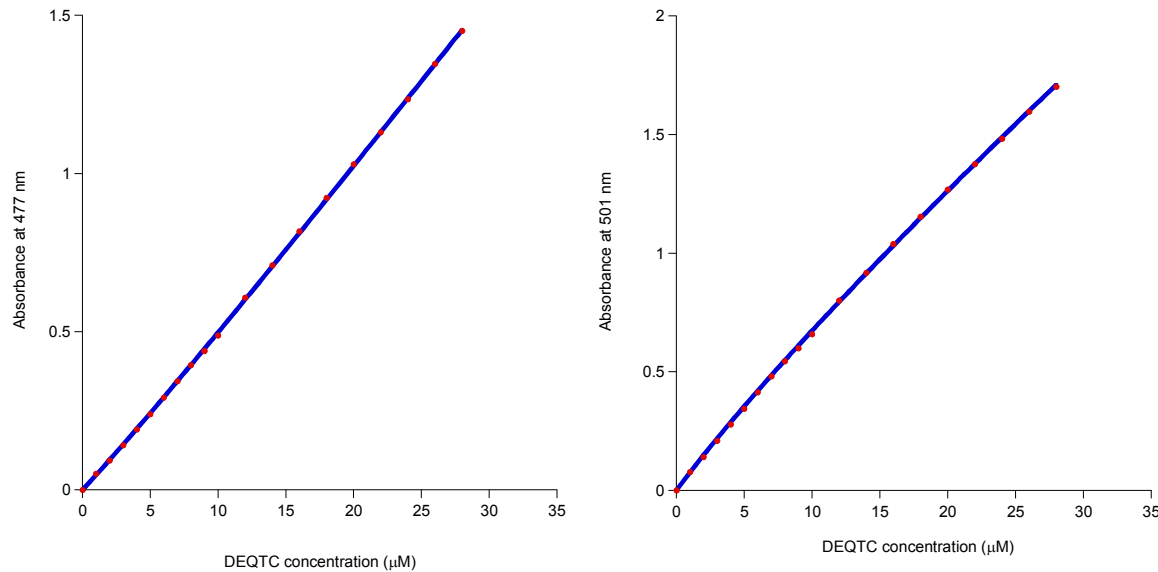


Figure S3: Beer-Lambert plots showing the absorption intensity at 477 nm (left) and at 501 nm (right) for DEQTC as a function of DEQTC concentration. Lines represent the regression analysis.

DEQTC		TO ⁺		
	ε_m (M ⁻¹ cm ⁻¹)	ε_d (M ⁻¹ cm ⁻¹)	ε_m (M ⁻¹ cm ⁻¹)	ε_d (M ⁻¹ cm ⁻¹)
477 nm	47000	120000	39000	126500
	±500	±2000	±400	±1500
501 nm	69500	98000	60500	100000
	±4000	±1500	±500	±2000
K_{eq}	$1.7 \pm 0.3 \times 10^4$ M ⁻¹		$2.5 \pm 0.2 \times 10^4$ M ⁻¹	

Table S1: Extinction coefficients and the equilibrium constant at 20°C for DEQTC and TO⁺ determined by using a regression analysis with Equation 8 and Datan software.

According to our data, the molar extinction coefficient of DEQTC monomer is larger than the one of TO⁺. This result is surprising since the two molecules possess the same chromophore. We thus tested if this difference is solvent dependent by performing a Beer-Lambert analysis in methanol, where the dyes are believed to exist in the monomeric form.

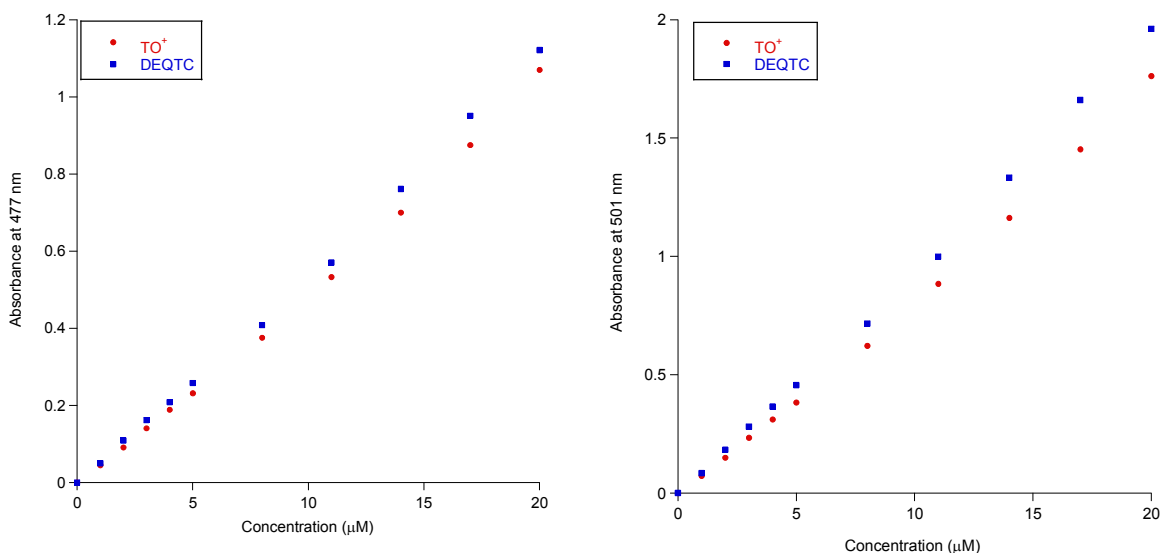


Figure S4: Beer-Lambert plot showing the absorption of DEQTC (blue square) and TO⁺ (red circle) solution in methanol at 477 nm (left) and 501 nm (right).

The molar extinction coefficients of these cyanine dyes in methanol are reported in Table S2, below. As shown in Figure S4, the molar extinction coefficient of TO^+ is also smaller in methanol than the one measured for DEQTC. Since both samples have different suppliers, we are attributing this result to a difference in purity between the two dyes.

	DEQTC ϵ (M ⁻¹ cm ⁻¹)	TO⁺ ϵ (M ⁻¹ cm ⁻¹)
477 nm	55000	51000
	±600	±700
501 nm	95000	84000
	±1000	±1200

Table S2: Molar extinction coefficient in methanol estimated using a linear regression analysis.

3. Assessment of the monomeric nature for 3,3-diethylthiacyanine iodide (THIA) and 1,1'-diethyl-2,2'-cyanine iodide (PIC)

Extinction coefficients were evaluated for 3,3-diethylthiacyanine iodide (THIA) and 1,1'-diethyl-2,2'-cyanine iodide (PIC) using the Beer-Lambert method, where THIA and PIC were assumed to be monomeric over the concentration range studied as to what has previously been reported in the literature.^{10, 11, 12, 13, 14, 15} The

concentration range for the Beer-Lambert analysis for both cyanine dyes was between 0 – 16 μM in order to have a final absorption maxima around 1.

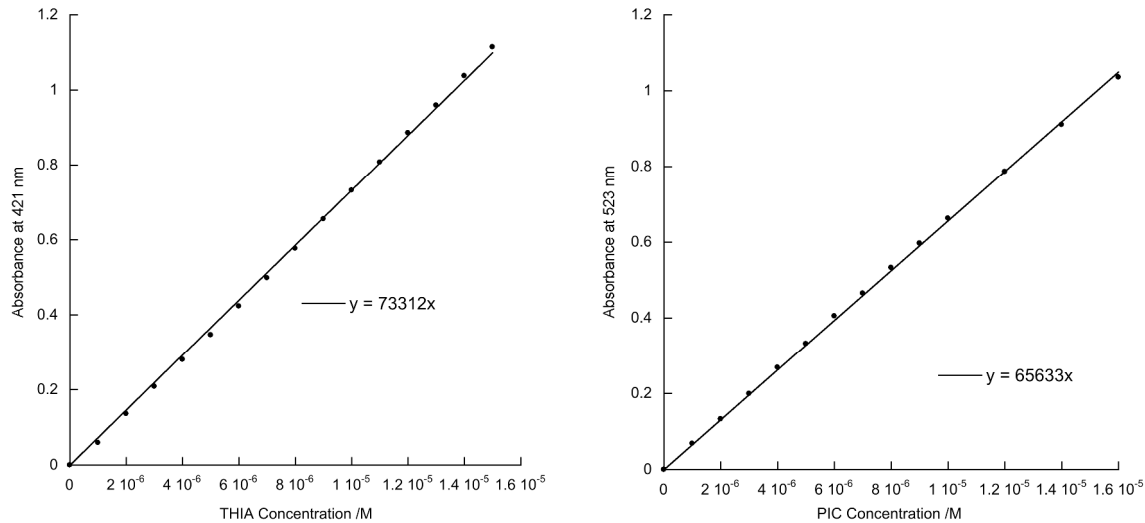


Figure S5: Beer-Lambert analysis for THIA at 421 nm (left) and PIC at 523 nm (right) where absorption intensity is plotted as a function of dye concentration. Values in the graphs represent a line of best fit with the slope being the extinction coefficient.

Although a linear Beer-Lambert analysis, of THIA and PIC, suggests that there is a single form a molecule present in solution, it is not enough evidence to claim that these dyes are purely monomeric in solution. For example, the Beer-Lambert analysis for DEQTC is also linear at 477 and 501 nm over a specific concentration range, yet as we have shown, both the monomeric and dimeric species are present for DEQTC at these concentrations.

If a dye is purely monomeric (M) in solution, the ratio of two absorption maxima at wavelengths (x and y) at a given concentration of the dye ($[M]$), can be simplified to the ratio of the molar extinction coefficients for the species at wavelengths x (ϵ_x) and y (ϵ_y) as shown below:

$$\frac{A^x}{A^y} = \frac{\varepsilon^x[M]l}{\varepsilon^y[M]l} = \frac{\varepsilon^x}{\varepsilon^y}. \text{ (Eq. 10)}$$

Therefore, this ratio will be constant at any concentration of the dye. However, if a dimeric species (D) also exist in solution, the ratio of the absorbance at different wavelengths, x and y , cannot be simplified to exclude the monomer or dimer ($[D]$) concentrations:

$$\frac{A^x}{A^y} = \frac{(\varepsilon_M^x[M] + \varepsilon_D^x[D])l}{(\varepsilon_M^y[M] + \varepsilon_D^y[D])l}. \text{ (Eq. 11)}$$

Therefore, when two species are absorbing light in solution, such as a monomer and dimer, the ratio of the absorbance at two chosen wavelengths will change as the concentration of the two species changes. Consequently, the presence of both a monomer and dimer of a dye in solution can be elucidated when a change in the ratio of two absorbing maxima is observed.

The ratio of the two absorption maxima for DEQTC, THIA, and PIC were calculated and then plotted as a function of dye concentration. As one can see from Figure S6, the peak ratio is only consistent for PIC and changes as a function of concentration for both DEQTC and THIA. This result is indicative that the peak at 404 nm is not simply due to a vibronic transition in THIA and may come from the absorption of light by a dimeric species, as seen in DEQTC.

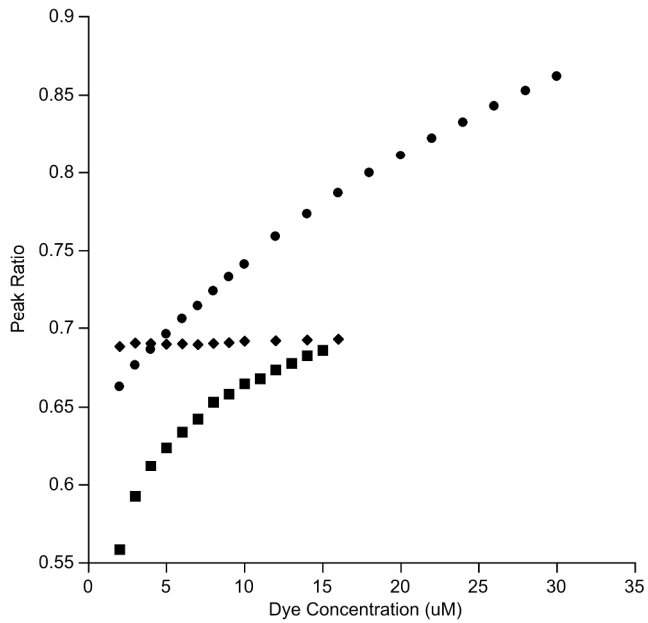
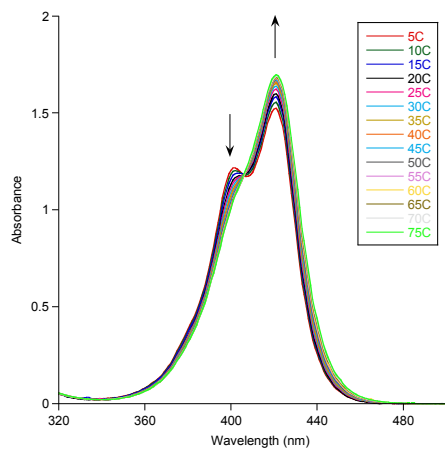


Figure S6: Peak ratios for DEQTC (absorbance at 477/absorbance at 501 nm, circle), THIA (absorbance at 404/absorbance at 421 nm, square), and PIC (absorbance at 491/absorbance at 523 nm, triangle) plotted as a function of dye concentration.

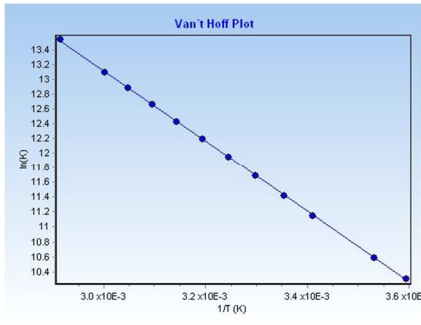
4. Chemometric approach in order to evaluate the equilibrium constant of THIA in aqueous solution.

The absorption spectrum of a 20 μM aqueous solution of THIA was recorded at different temperatures ranging from 5°C to 75°C (278.15K - 348.15K). The sample was kept in a plastic cuvette in order to minimize the adsorption of the dye on the surface of the cuvette. The data were then corrected for thermal expansion of the water (see section above) and analyzed simultaneously with the datan software.

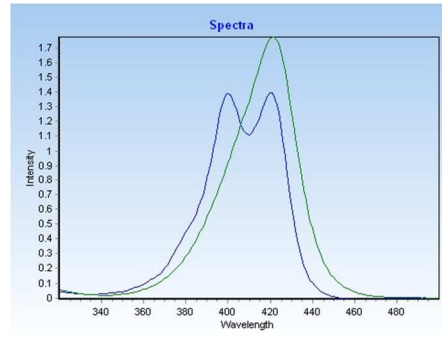
a)



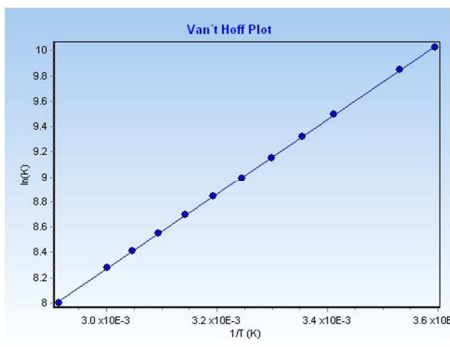
b)



c)



d)



e)

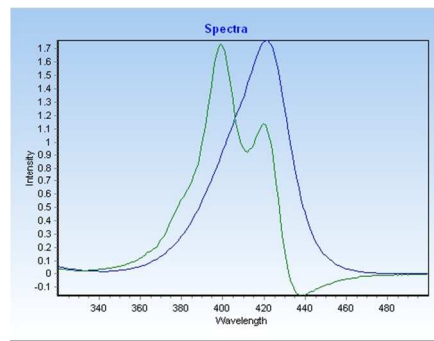


Figure S7: a) Absorption spectra of a 20 μM aqueous solution of THIA recorded between 5°C and 75°C. The absorption spectra have been corrected for thermal expansion of water. Arrows demonstrate the movement of the absorption spectra when the temperature is increased, highlighting the change in the absorption intensities of the monomer and dimer as the temperature increased. b) Initial Van't Hoff plot in 5K interval between 278.15K and 348.15K with the c) corresponding calculated absorption spectra for the monomer (blue) and dimer (green) of THIA (20 μM). d) Van't Hoff plot in 5K interval between

278.15K and 348.15K when both ΔH and ΔS are kept negative and e) the corresponding calculated absorption spectra for the monomer (blue) and dimer (green) of THIA (20 μ M).

The initial solution provided by the software was rejected as both ΔH and ΔS were found to be positive (Figure S7b). Indeed, aggregation is known to be an enthalpy driven process, which translates in both ΔH and ΔS being negative.¹⁶ When these thermodynamic parameters were forced to have negative values, our data converges towards another solution with acceptable variation of K_{eq} in function of the temperature (Figure 7d), providing a value of K_{eq} at 20°C of $1.4 \pm 0.1 \times 10^4$ M⁻¹. However, this solution was also rejected as the calculated absorption spectrum for the dimeric form of THIA has negative absorption values (Figure S7e).

5. DFT calculation of the various cyanine dyes employed in this study.

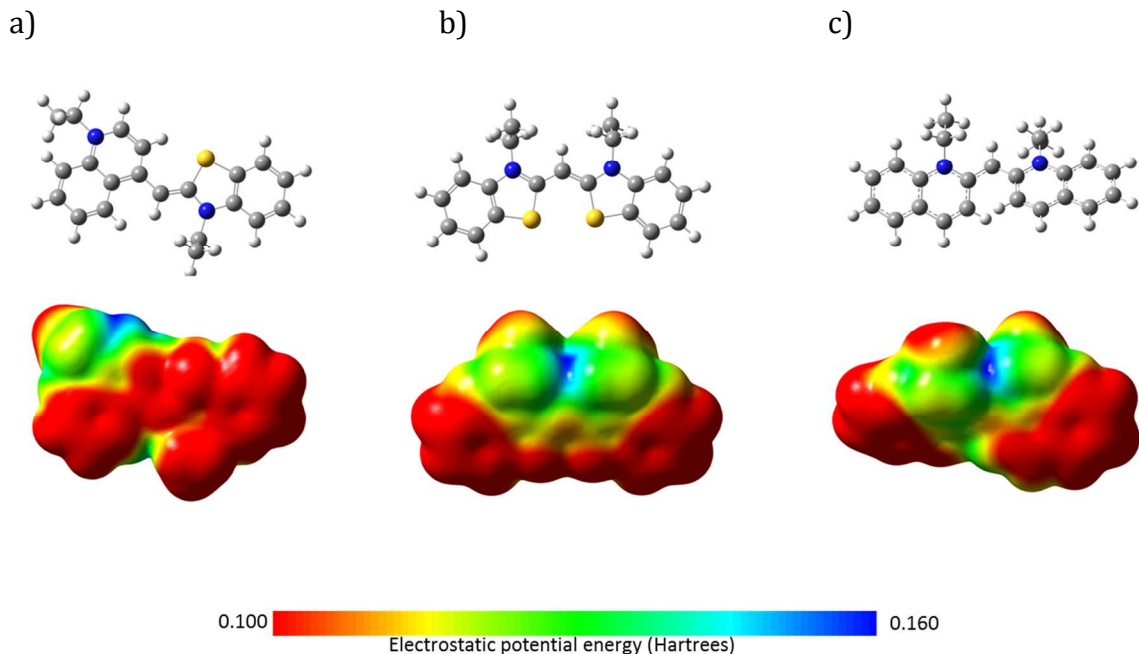
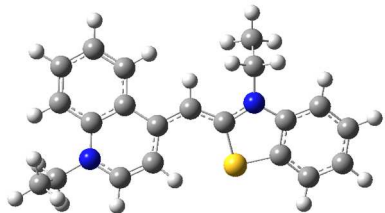


Figure S8: Optimized structures (above) and electrostatic potential maps (below) calculated at the B3LYP/6-31+g(d) level for (a) DEQTC, (b) PIC, and (c) THIA cations.

All calculations were performed with the Gaussian 09 program,¹⁷ and all images were generated with Gauss View. Optimizations and frequency calculations were performed at the B3LYP/6-31+G(d) level, and frequency calculations showed all structures to be minima on the potential energy surface. The Polarizable Continuum Model (PCM) was used to include the effects of solvation in water in each calculation. Iodine atoms were treated separately with the LANL2DZ pseudopotential. The Cartesian coordinates and HF energies of the optimized structures are listed below:

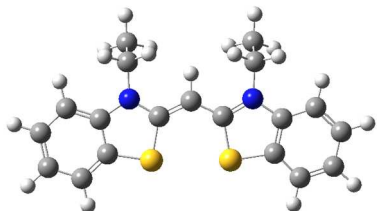
DEQTC⁺: HF = -1320.47856762 a.u.



Symbol	X	Y	Z
C	-6.1192560	-0.1861540	-0.1241770
C	-5.0372800	0.6725410	-0.3250980
C	-3.7422730	0.1556630	-0.1891800
C	-3.5596450	-1.1935150	0.1517350
C	-4.6388200	-2.0536670	0.3501180
C	-5.9281330	-1.5357990	0.2082970
N	-2.5323500	0.8380450	-0.3620930
C	-1.4042230	0.0914800	-0.1303160
S	-1.8465440	-1.5679660	0.2757720
C	-0.1134710	0.6229520	-0.1673520
C	1.1397530	-0.0229090	-0.0407620
C	2.3724450	0.7618130	0.0685890
C	3.6387210	0.1068940	0.1861880
N	3.6981010	-1.2866820	0.2054920
C	2.5591740	-2.0005090	0.0937660
C	1.3156260	-1.4280120	-0.0258190
C	2.3733560	2.1793060	0.0793640
C	3.5394310	2.9139750	0.1836380
C	4.7745570	2.2512380	0.2877270
C	4.8242160	0.8694430	0.2907610
C	4.9834030	-2.0243630	0.2968740

C	5.7011730	-2.1461180	-1.0481860
C	-2.4999390	2.2588390	-0.7597860
C	-2.5103490	3.2149820	0.4349200
H	-7.1269860	0.2055080	-0.2258470
H	-5.2094190	1.7138430	-0.5724140
H	-4.4795660	-3.0956220	0.6095860
H	-6.7858040	-2.1840030	0.3602410
H	-0.0878920	1.6940980	-0.2906890
H	2.6744390	-3.0779880	0.0948480
H	0.4867770	-2.1100410	-0.1460820
H	1.4380460	2.7200560	0.0119060
H	3.4973550	3.9987980	0.1884400
H	5.6966290	2.8189810	0.3689150
H	5.7866670	0.3820780	0.3712810
H	4.7398610	-3.0142590	0.6866640
H	5.6059950	-1.5368980	1.0490030
H	6.6286420	-2.7110270	-0.9055490
H	5.0801900	-2.6833360	-1.7724950
H	5.9581890	-1.1696150	-1.4693580
H	-3.3663670	2.4276560	-1.4024710
H	-1.6205030	2.4102680	-1.3882460
H	-1.6361700	3.0648720	1.0763170
H	-3.4108560	3.0786230	1.0422550
H	-2.4955750	4.2474480	0.0697360

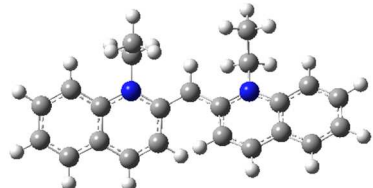
THIA⁺: HF = -1641.24829229 a.u.



Symbol	X	Y	Z
C	-5.6291869	-1.7784670	-0.1488337
C	-5.9285094	-0.4178444	0.0217422
C	-4.9201582	0.5349472	0.1695068
C	-3.5882077	0.1018490	0.1457789
C	-3.2973548	-1.2594349	-0.0321997
C	-4.3034043	-2.2139407	-0.1787147
N	-2.4350813	0.8860341	0.2854143
C	-1.2598695	0.1970736	0.1906035
S	-1.5580360	-1.5202964	-0.0398970
C	-2.5088370	2.3470750	0.4903533
C	-2.4780092	3.1349519	-0.8206720
C	0.0003043	0.8020421	0.2649203
C	1.2593197	0.1949659	0.1883503
N	2.4353677	0.8797601	0.3005743
C	3.5875317	0.0966270	0.1479845
C	3.2949761	-1.2606296	-0.0559262

S	1.5552093	-1.5182839	-0.0738153
C	2.5112517	2.3343286	0.5473634
C	2.4886762	3.1605014	-0.7400159
C	4.9199936	0.5272832	0.1825224
C	5.9272834	-0.4241218	0.0193554
C	5.6263101	-1.7809015	-0.1770036
C	4.2999548	-2.2138097	-0.2177543
H	-6.4323329	-2.5002269	-0.2617618
H	-6.9645908	-0.0932553	0.0373056
H	-5.1756257	1.5812613	0.2917846
H	-4.0614010	-3.2633622	-0.3128151
H	-1.6907714	2.6349373	1.1530310
H	-3.4289156	2.5419487	1.0439004
H	-3.3247886	2.8697431	-1.4615665
H	-1.5531427	2.9533603	-1.3771947
H	-2.5391690	4.2051112	-0.5964642
H	0.0017721	1.8764153	0.3732761
H	3.4290525	2.5106682	1.1108872
H	1.6900255	2.6042728	1.2138733
H	3.3339639	2.9072399	-1.3876429
H	2.5581036	4.2231012	-0.4845261
H	1.5629465	3.0029185	-1.3021159
H	5.1765356	1.5709026	0.3240500
H	6.9637955	-0.1014049	0.0429610
H	6.4286052	-2.5016928	-0.3015805
H	4.0567731	-3.2601849	-0.3720920

PIC⁺: HF = -999.70114720 a.u.



Symbol	X	Y	Z
C	-6.2469071	-1.1578767	-0.1064116
C	-5.1113912	-1.8827006	-0.4245746
C	-3.8352104	-1.2802961	-0.3984328
C	-3.7027166	0.0960034	-0.0615001
C	-4.8706567	0.8174331	0.2738858
C	-6.1127936	0.1948804	0.2500348
H	-2.7435482	-3.0481035	-1.0400630
H	-7.2257120	-1.6271760	-0.1239456
H	-5.1806489	-2.9324343	-0.6972570
C	-2.6530539	-2.0139869	-0.7191661
H	-4.8301094	1.8542443	0.5778556
H	-6.9913424	0.7736470	0.5204588
C	-1.2723318	-0.0481746	-0.2556962
C	-1.4317643	-1.4253917	-0.6416395
H	-0.5476233	-1.9769072	-0.9319740
C	-0.0012726	0.5576301	-0.1722564

N	-2.4293343	0.6881374	-0.0552966
C	-2.3323487	2.1447499	0.2091380
H	-1.5316551	2.5473377	-0.4105812
H	-3.2405176	2.6091378	-0.1699487
C	-2.1143476	2.4756845	1.6864114
H	-2.9438015	2.1112173	2.3010282
H	-1.1868200	2.0327246	2.0621198
H	-2.0496334	3.5624550	1.8065445
C	1.2438094	-0.1080392	-0.0194099
C	1.3652315	-1.3764520	0.6376689
C	2.5770735	-1.9533626	0.8633600
H	0.4662901	-1.8406371	1.0204134
C	3.6773753	-0.0210464	-0.1557451
C	3.7796996	-1.2940657	0.4718991
H	2.6422739	-2.9040234	1.3854438
C	4.8662297	0.6610580	-0.4974638
C	5.0516557	-1.8562742	0.7203303
C	6.1024667	0.0815796	-0.2429553
H	4.8436245	1.6434058	-0.9488274
C	6.2065270	-1.1833128	0.3636120
H	5.1011469	-2.8298852	1.2003861
H	7.0015993	0.6262977	-0.5161010
H	7.1817127	-1.6202711	0.5552141
H	0.0425194	1.6336717	-0.1810627
N	2.4093021	0.5134723	-0.4241063
C	2.3238906	1.7662738	-1.2157197
H	3.1192677	1.7358157	-1.9611031
H	1.3849831	1.7268408	-1.7695711
C	2.4119511	3.0393160	-0.3702102
H	1.5989358	3.1013651	0.3599785
H	3.3582088	3.0975865	0.1763232
H	2.3443821	3.9106470	-1.0304662

6. Evaluation of the DEQTC percent monomer composition before and after the addition of sodium acetate (NaCH_3CO_2), sodium chloride (NaCl), or sodium bromide (NaBr).

Comparing the percentage of monomer before and after the addition of salt is a simple way to observe a change in the monomer-dimer equilibrium. In order to do so, the mole fraction of the monomer can be elucidated from absorption spectroscopy. Depending on the total concentration of DEQTC in solution, the concentration of

monomer and dimer can be represented in the following rearrangement of Equation 5, where χ , the mole fraction of the monomer is incorporated;

$$[DEQTC] = \chi C_T, \text{ (Eq. 12)}$$

$$[(DEQTC)_2] = \frac{(1-\chi)}{2} C_T. \text{ (Eq. 13)}$$

The absorbance at a given wavelength, λ , similarly to Equation 9, can also be expressed in terms of these concentrations along with the mole fraction of the monomer:

$$A^\lambda = (\varepsilon_m^\lambda \chi C_T + \varepsilon_d^\lambda \frac{(1-\chi)}{2} C_T)l. \text{ (Eq. 14)}$$

Then, the ratio of absorbance of the dimer and monomer, $A^{477}/A^{501} = R$ (a constant at a given C_T) can be used to simplify for χ ;

$$\frac{A^{477}}{A^{501}} = \frac{2\varepsilon_m^{477} \chi C_T + \varepsilon_d^{477} (1-\chi) C_T}{2\varepsilon_m^{501} \chi C_T + \varepsilon_d^{501} (1-\chi) C_T}, \text{ (Eq. 15)}$$

$$\chi = \frac{\varepsilon_d^{477} - R\varepsilon_d^{501}}{2(R\varepsilon_m^{501} - \varepsilon_m^{477}) + (\varepsilon_d^{477} - R\varepsilon_d^{501})}. \text{ (Eq. 16)}$$

Once the mole fraction for the monomer is known, χ , the percentage of monomer can simply be determined at individual salt concentrations (Table S2) as follows:

$$\%monomer = \frac{[DEQTC]}{C_T} \bullet 100\%. \text{ (Eq. 17)}$$

	No salt added	NaCH ₃ CO ₂	NaCl	NaBr
% Monomer	69%	61%	55%	50%

Table S3: Percentage of the monomeric form of DEQTC in the absence of added salt or in the presence of 250 mM of NaCH₃CO₂, NaCl or NaBr.

7. Quantification of the equilibrium constant for DEQTC upon the addition of NaCH₃CO₂, NaCl, and NaBr.

By knowing the mole fraction of the monomers at certain added salt concentrations, the equilibrium constant, at each salt concentration, can be determined with Equation 2 (Figure S9).

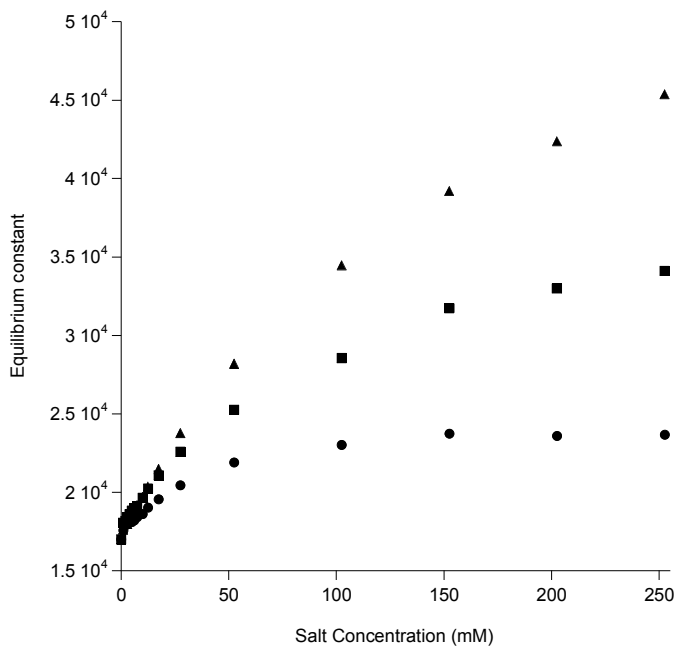


Figure S9: Mathematically determined K_{eq} of DEQTC in aqueous solution plotted as a function of added salt concentration of NaCH_3CO_2 (circles), NaCl (squares), and NaBr (triangles).

8. Absorption spectra of THIA before and after the addition of NaCH_3CO_2 , NaCl , or NaBr .

As shown in all graphs in Figure S10 the addition of NaCH_3CO_2 , NaCl , and NaBr to an aqueous solution of THIA results in a decrease in the absorption intensity of the monomer peak at 421 nm. Along with this decrease there is also a slight increase in the peak at 404 nm, which we have characterized as containing contribution from the dimeric species. This increase is most pronounced for NaBr and least pronounced for NaCH_3CO_2 .

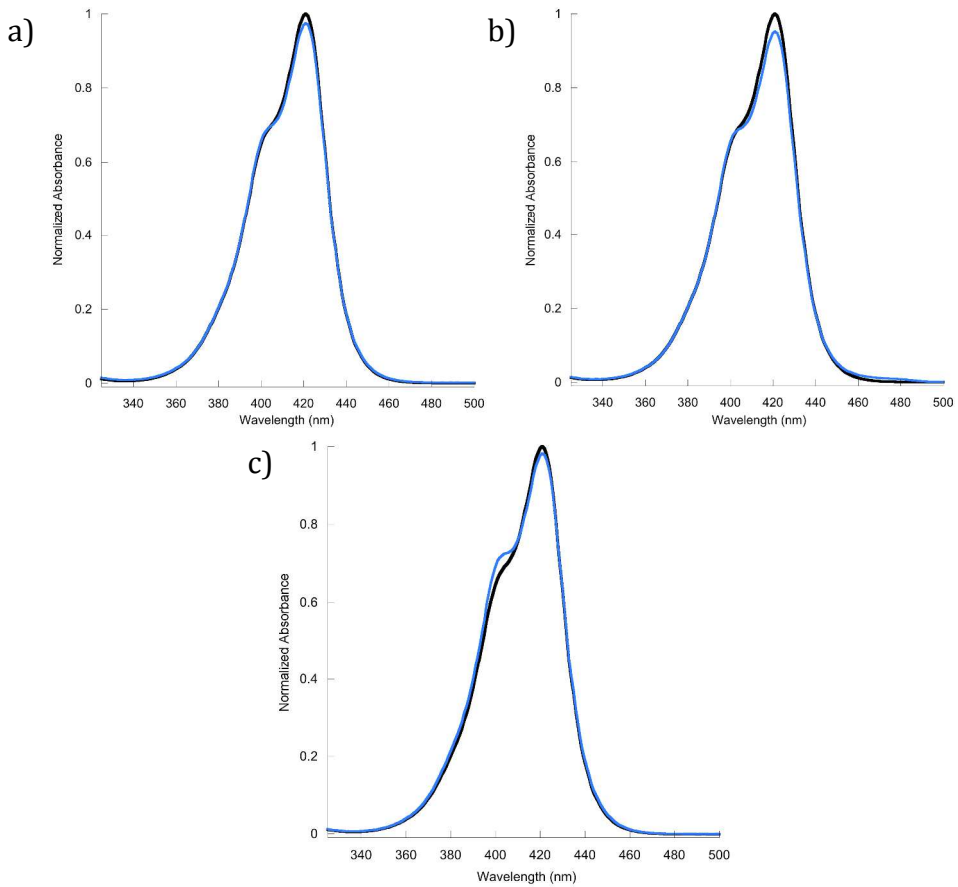


Figure S10: Absorption spectra of THIA before (black trace) after (blue trace) the addition of 125 mM of NaCH_3CO_2 (a), NaCl (b), and NaBr (c).

9. Absorption of PIC before and after the addition of NaBr.

In order to assess what occurs when small monovalent salts are added to dye solutions consisting of only the monomeric form of a dye, a 10 μM solution of PIC was prepared. Figure S11 shows the absorption spectrum of PIC before and after the addition of NaBr. Results for NaCH_3CO_2 and NaCl are not shown as they display the same results as for when NaBr is used.

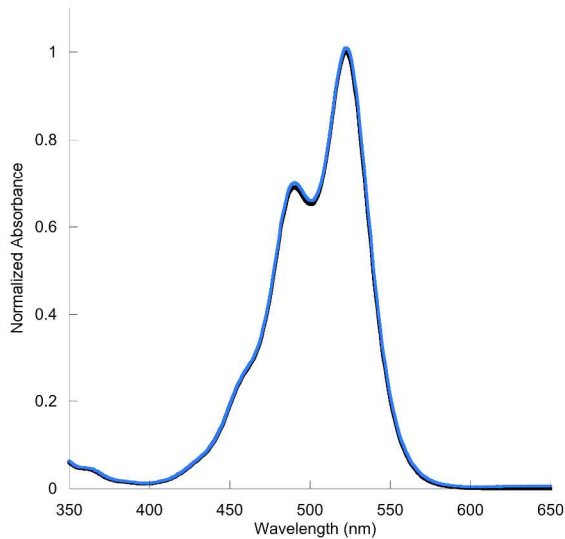


Figure S11: 10 μ M solution of PIC (black trace) with 125 mM final concentration of NaBr (blue trace).

10. Absorption spectra recorded for the addition of sodium iodide (NaI) and sodium tetrafluoroborate (NaBF₄) to a solution of DEQTC, THIA and PIC.

As shown in Figure S12, the addition of NaI and NaBF₄ to an aqueous solution of DEQTC results in a decrease in the absorption intensity of both the monomer and dimer peaks with increasing salt concentration. In addition, at high salt concentrations, there is also an increase in absorption intensity both red and blue shifted compared to that of the monomer.

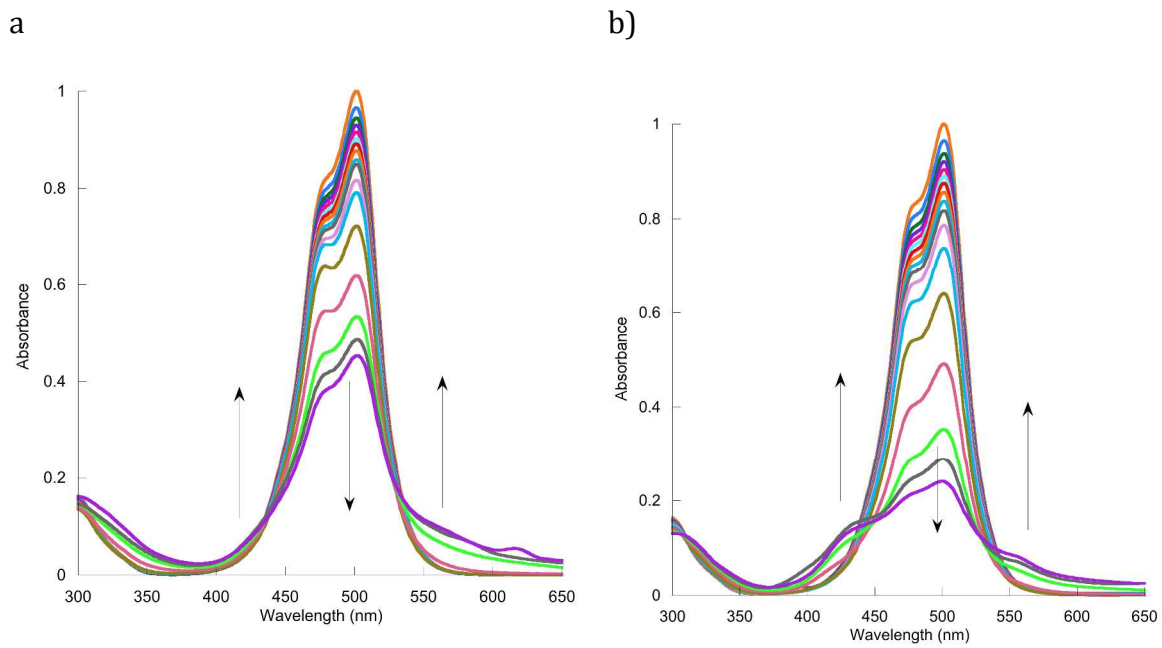


Figure S12: Absorption spectrum of a 20 μM solution of DEQTC with the consecutive additions of NaI (a) and NaBF₄ (b) up to a final concentration of 250 mM. Arrows show the progression of the absorption spectra.

The same behavior is also observed for an aqueous solution of THIA upon addition of NaI and NaBF₄.

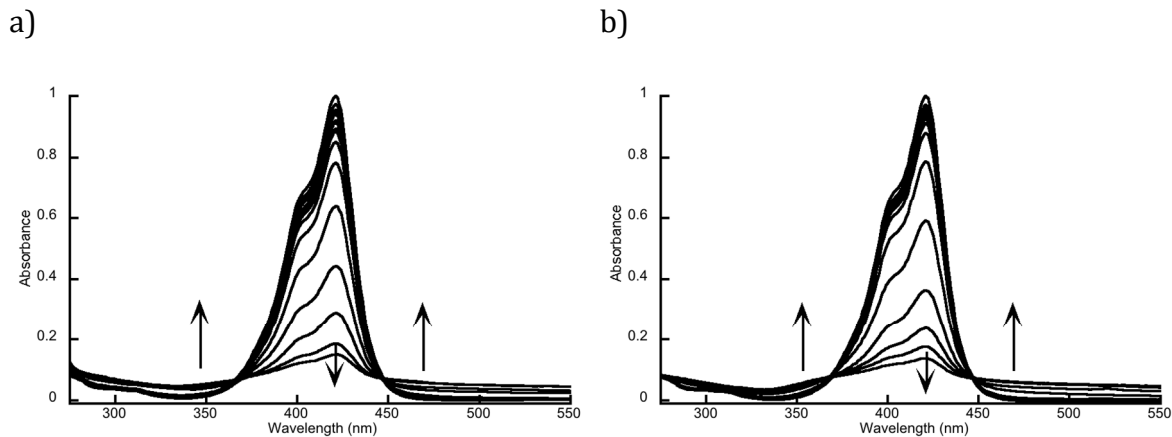


Figure S13: Evolution of the absorption spectra of a 10 μM solution of THIA in water with the additions NaI (a), NaBF₄ (b) and NaClO₄ (c) added up to a concentration of 125 mM.

On the contrary, PIC does display negligible changes of its absorption spectrum upon addition of NaI, while an important decrease of the absorption maximum is seen with the addition of NaBF₄.

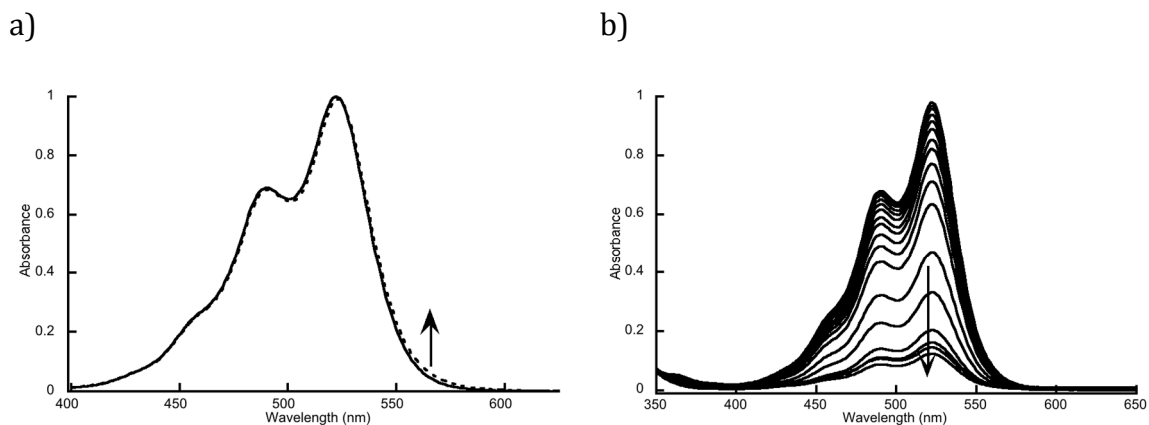
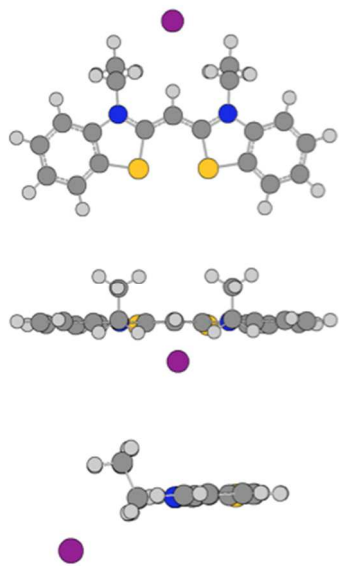


Figure S14: Evolution of the absorption spectra of a 10 μM solution of PIC in water with the additions NaI (a) and NaBF₄ (b) added up to a concentration of 125 mM.

11. DFT Calculation for the ion pairs

As shown in Figure S15, the ion pair of THIA with I^- prefers a geometry where the ethyl groups are turned in the same direction, while the spherical I^- anion resides out of the molecular plane. In contrast, the tetrahedral BF_4^- anions fit closer into the region of high positive electrostatic potential on the THIA cation localized on the polymethine backbone.

a)



b)

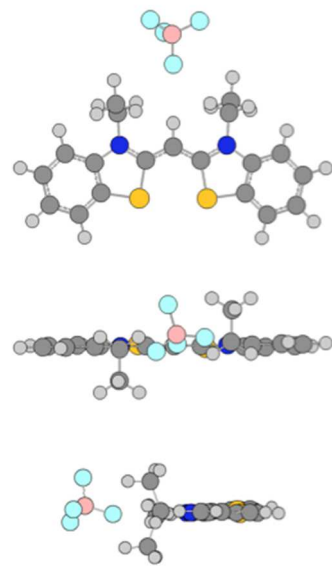


Figure S15: Optimized structures at the B3LYP/6-31+g(d) level of ion pairs of THIA with (a) I^- and (b) BF_4^- .

Below are the results of the DFT calculation on the formation of ion pairs between DEQTC and I^- , BF_4^- and ClO_4^- , showing interaction of the anion with the quinolium moiety of DEQTC.

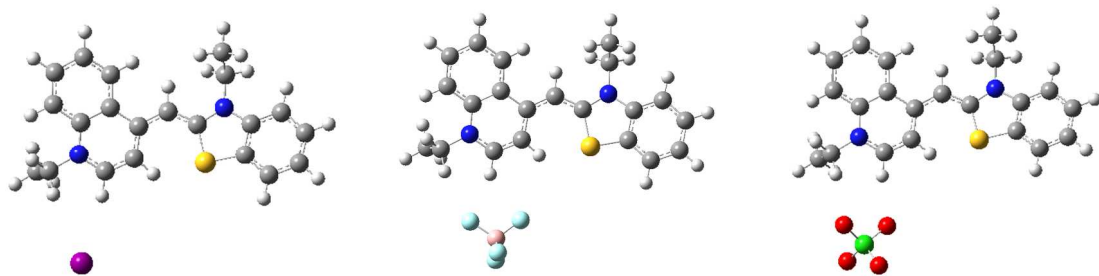


Figure S16: Optimized structures calculated at the B3LYP/6-31+g(d) level for DEQTC ion pair with I^- (left), BF_4^- (middle) and ClO_4^- (right) as counter ion.

Results obtained for PIC are shown in Figure S17 below.

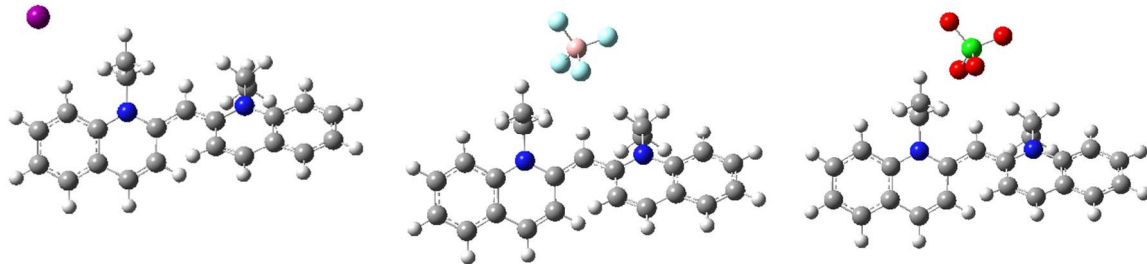
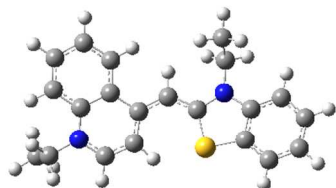


Figure S17: Optimized structures calculated at the B3LYP/6-31+g(d) level for PIC ion pair with I^- (left), BF_4^- (middle) and ClO_4^- (right) as counter ion.

All calculations were performed with the Gaussian 09 program,¹⁷ and all images were generated with Gauss View. Optimizations and frequency calculations were performed at the B3LYP/6-31+G(d) level, and frequency calculations showed all structures to be minima on the potential energy surface. The Polarizable Continuum Model (PCM) was used to include the effects of solvation in water in each calculation. Iodine atoms were treated separately with the LANL2DZ

pseudopotential. The Cartesian coordinates and HF energies of the optimized structures are listed below:

DEQTC⁺ I⁻: HF = -1332.03762119 a.u.

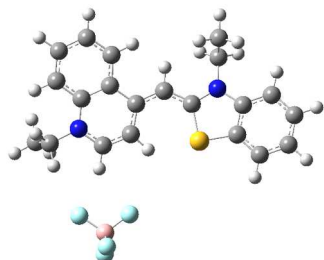


•

Symbol	X	Y	Z
C	-6.5731702	-2.4576613	0.1111930
C	-6.0813398	-1.1614415	0.2779797
C	-4.6983966	-0.9562834	0.1846656
C	-3.8458944	-2.0398966	-0.0797988
C	-4.3347008	-3.3355167	-0.2440362
C	-5.7138541	-3.5369074	-0.1456283
N	-4.0070863	0.2514135	0.3340816
C	-2.6477708	0.1710300	0.1535703
S	-2.1747919	-1.5003378	-0.1618921
C	-1.8064105	1.2837899	0.1660017
C	-0.3920542	1.3525781	0.0939098
C	0.2801353	2.6408046	-0.0901066
C	1.7083904	2.7104747	-0.1284775
N	2.4617601	1.5442075	-0.0007271
C	1.8361391	0.3605224	0.1628397
C	0.4664535	0.2339573	0.2090541
C	-0.4332332	3.8548142	-0.2571454
C	0.2083443	5.0668451	-0.4321924
C	1.6135599	5.1160172	-0.4530988
C	2.3527402	3.9565003	-0.3053858
H	-7.6436788	-2.6267316	0.1798131
H	-6.7645957	-0.3412683	0.4671383
H	-3.6615827	-4.1630457	-0.4452915
H	-6.1200801	-4.5358242	-0.2722708
H	-2.3296257	2.2257187	0.2195477
H	2.4824194	-0.5076956	0.2590378
H	0.0861776	-0.7617572	0.3859093
H	-1.5156925	3.8475900	-0.2622762
H	-0.3736812	5.9745975	-0.5584386
H	2.1270217	6.0631885	-0.5891290
H	3.4325232	4.0181367	-0.3267137
C	3.9470823	1.5548827	0.0080514
H	4.2911598	2.2134999	-0.7918749
H	4.2599022	0.5408444	-0.2518552
C	-4.7106224	1.5062948	0.6597013
H	-4.0477397	2.1088772	1.2837386
H	-5.5617895	1.2379822	1.2892224

I	4.6327813	-2.6550234	-0.1290721
C	4.5310329	1.9512445	1.3654416
H	5.6243509	1.9172576	1.3046827
H	4.2379087	2.9615519	1.6670395
H	4.2101747	1.2512185	2.1441655
C	-5.1701537	2.2770057	-0.5804363
H	-5.8596449	1.6790459	-1.1853163
H	-5.6914417	3.1874513	-0.2656044
H	-4.3232026	2.5673329	-1.2105284

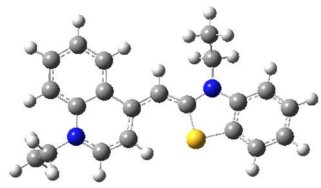
DEQTC⁺ BF₄⁻: HF = -1745.14051883 a.u.



Symbol	X	Y	Z
C	6.4133254	1.6056844	0.1493793
C	5.7397494	0.3940909	0.3144717
C	4.3436394	0.3866538	0.1982491
C	3.6587365	1.5775037	-0.0897234
C	4.3293157	2.7888670	-0.2525749
C	5.7207208	2.7934830	-0.1292734
N	3.4851588	-0.7089094	0.3448581
C	2.1541987	-0.4381583	0.1416677
S	1.9288784	1.2797637	-0.1981636
C	1.1622188	-1.4188309	0.1557725
C	-0.2458571	-1.2891764	0.0604618
C	-1.0897952	-2.4761804	-0.0973365
C	-2.5133812	-2.3487468	-0.1500519
N	-3.0975410	-1.0854905	-0.0674548
C	-2.3137564	0.0041694	0.0635565
C	-0.9409217	-0.0587249	0.1255158
C	-0.5507294	-3.7812185	-0.2239668
C	-1.3524842	-4.8972860	-0.3721582
C	-2.7503820	-4.7525937	-0.4048886
C	-3.3225743	-3.4983505	-0.2978087
H	7.4956920	1.6215133	0.2363614
H	6.2966098	-0.5132878	0.5190673
H	3.7841958	3.7019047	-0.4710411
H	6.2666537	3.7237250	-0.2539815
H	1.5442105	-2.4243414	0.2363061
H	-2.8275857	0.9565102	0.1253029
H	-0.4312984	0.8826384	0.2712044
H	0.5223812	-3.9236110	-0.2187715
H	-0.9007966	-5.8798761	-0.4681072
H	-3.3892081	-5.6232385	-0.5191942
H	-4.4004002	-3.4111622	-0.3286422

C	-4.5698168	-0.8895722	-0.0710959
H	-4.9992373	-1.5206881	-0.8514636
H	-4.7366218	0.1462806	-0.3698551
C	3.9985985	-2.0483245	0.6892213
H	3.2490762	-2.5450367	1.3080031
H	4.8709532	-1.8980122	1.3286404
F	-3.6345685	4.4242185	-1.3922570
F	-2.2125932	3.3867139	0.1032246
F	-4.4002187	2.6820907	-0.0821034
F	-3.9255646	4.7293805	0.8774533
B	-3.5430445	3.8114120	-0.1239010
C	-5.2086606	-1.1544383	1.2933881
H	-6.2879859	-0.9827784	1.2197398
H	-5.0492058	-2.1821792	1.6330440
H	-4.8038008	-0.4731997	2.0490009
C	4.3594115	-2.8854965	-0.5399319
H	5.1393050	-2.3986051	-1.1341962
H	4.7351138	-3.8613587	-0.2141734
H	3.4889628	-3.0494354	-1.1830435

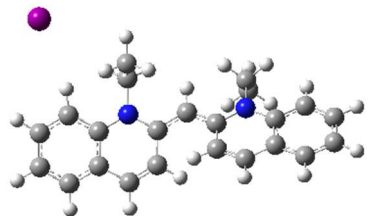
DEQTC⁺ ClO₄⁻: HF = -2081.40053036 a.u.



Symbol	X	Y	Z
C	6.4976336	-2.5324716	-0.0955637
C	6.0168704	-1.2370329	-0.2948674
C	4.6383302	-1.0137099	-0.1848853
C	3.7793164	-2.0784485	0.1289784
C	4.2569652	-3.3733181	0.3253931
C	5.6316182	-3.5931509	0.2096767
N	3.9575310	0.1962241	-0.3615685
C	2.6015527	0.1378248	-0.1541623
S	2.1152173	-1.5176615	0.2229029
C	1.7731653	1.2597512	-0.1824829
C	0.3615033	1.3451376	-0.0885594
C	-0.2952957	2.6418982	0.0872444
C	-1.7215171	2.7243801	0.1593763
N	-2.4871427	1.5622086	0.0732029
C	-1.8756830	0.3720429	-0.0965344
C	-0.5091099	0.2335914	-0.1756672
C	0.4320252	3.8523237	0.2124853
C	-0.1946611	5.0730726	0.3773256
C	-1.5981489	5.1351682	0.4299337
C	-2.3502571	3.9796697	0.3250998
H	7.5649552	-2.7155415	-0.1768369

H	6.7051766	-0.4305217	-0.5207949
H	3.5785252	-4.1864035	0.5642353
H	6.0291918	-4.5921761	0.3607061
H	2.3062285	2.1940737	-0.2650626
H	-2.5260897	-0.4924080	-0.1830605
H	-0.1410426	-0.7660568	-0.3566196
H	1.5142006	3.8353014	0.1909843
H	0.3978698	5.9780215	0.4705499
H	-2.1004260	6.0895795	0.5567832
H	-3.4286767	4.0526166	0.3683315
C	-3.9717791	1.5853770	0.1144524
H	-4.2813940	2.2776276	0.8995168
H	-4.2854798	0.5887457	0.4300872
C	4.6681257	1.4314144	-0.7427912
H	3.9988062	2.0199631	-1.3732656
H	5.5030857	1.1320633	-1.3798811
Cl	-4.8744443	-2.7999595	0.0785324
O	-4.8020877	-4.1209818	0.7885208
O	-3.5526692	-2.5125614	-0.5822502
O	-5.9546045	-2.8467413	-0.9634289
O	-5.1772562	-1.7104222	1.0691358
C	-4.5985875	1.9378215	-1.2356572
H	-5.6892732	1.9268433	-1.1350528
H	-4.2985864	2.9303258	-1.5856447
H	-4.3178710	1.2029153	-1.9973850
C	5.1612736	2.2374185	0.4609937
H	5.8563625	1.6519305	1.0714410
H	5.6858020	3.1307283	0.1053903
H	4.3308919	2.5583322	1.0980903

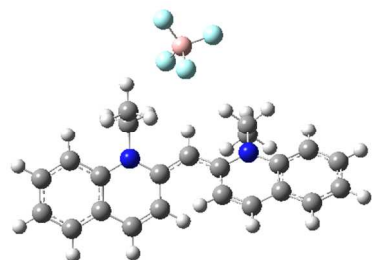
PIC⁺ I: HF = -1011.25778243 a.u.



Symbol	X	Y	Z
C	7.8613864	0.5763199	0.6397319
C	6.9637347	-0.3818232	1.0794489
C	5.5868426	-0.2746270	0.7865210
C	5.0986311	0.8408282	0.0495655
C	6.0309598	1.8010765	-0.4054596
C	7.3826690	1.6629676	-0.1124844
H	4.9941408	-2.0839197	1.8383294
H	8.9198156	0.4869398	0.8641383
H	7.3038033	-1.2386099	1.6551704
C	4.6480648	-1.2588806	1.2218563
H	5.7268386	2.6459760	-1.0076633
H	8.0758630	2.4129263	-0.4825999
C	2.8275172	-0.0587374	0.1089710

C	3.3357165	-1.1587506	0.8860306
H	2.6265440	-1.8836998	1.2619253
C	1.4584268	0.0509913	-0.2183882
N	3.7239201	0.9471173	-0.2184008
C	0.5206912	-1.0114530	-0.2728009
C	0.9284521	-2.3626231	-0.5397558
C	0.0317548	-3.3809368	-0.6262281
H	1.9750701	-2.5463462	-0.7417646
C	-1.7887161	-1.7994829	-0.2072616
C	-1.3606009	-3.1385580	-0.4363789
H	0.3666018	-4.3877217	-0.8603352
C	-3.1677618	-1.5620474	-0.0049240
C	-2.3066060	-4.1866290	-0.4855828
C	-4.0721197	-2.6157453	-0.0489381
H	-3.5608988	-0.5736066	0.1980088
C	-3.6537342	-3.9359465	-0.2943422
H	-1.9491090	-5.1956209	-0.6731823
H	-5.1248042	-2.4030569	0.1148699
H	-4.3774293	-4.7445850	-0.3287194
H	1.0871103	1.0334593	-0.4538682
N	-0.8370165	-0.7664544	-0.1701701
C	-1.3119788	0.6220524	0.0658935
H	-0.7133473	1.2974643	-0.5433846
H	-2.3226895	0.7071746	-0.3261326
C	3.2388160	2.1607985	-0.9207337
H	2.2609973	2.4196438	-0.5176652
H	3.8860859	2.9880290	-0.6364697
I	-5.5882177	1.8684304	0.1863974
C	3.1864489	1.9901588	-2.4400308
H	2.8173424	2.9154638	-2.8955045
H	4.1796054	1.7779735	-2.8493360
H	2.5144898	1.1747296	-2.7255951
C	-1.2633808	1.0125542	1.5438588
H	-1.8997908	0.3546722	2.1448679
H	-0.2430044	0.9630703	1.9366541
H	-1.6273035	2.0391541	1.6577809

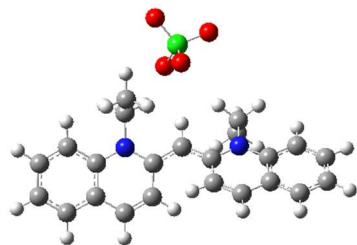
PIC⁺ BF₄⁻: HF = -1424.35974756 a.u.



Symbol	X	Y	Z
--------	---	---	---

C	-6.0953909	-2.4207602	-0.4330103
C	-4.9090444	-2.9972135	-0.8517470
C	-3.6728799	-2.3494121	-0.6388152
C	-3.6339434	-1.0753659	-0.0051674
C	-4.8540891	-0.5079822	0.4282252
C	-6.0545168	-1.1742652	0.2152954
H	-2.4567287	-3.8775271	-1.5938865
H	-7.0431017	-2.9249242	-0.5952578
H	-4.9061338	-3.9636115	-1.3490032
C	-2.4396317	-2.9335976	-1.0560639
H	-4.8858986	0.4380493	0.9503409
H	-6.9746586	-0.7154899	0.5657761
C	-1.1960976	-1.0373795	-0.1361147
C	-1.2598160	-2.3088250	-0.8052644
H	-0.3358960	-2.7341470	-1.1734756
C	0.0366908	-0.3804073	0.0886808
N	-2.3995924	-0.4340221	0.1877618
C	1.3027404	-1.0056631	0.1889730
C	1.4336806	-2.3763561	0.6036415
C	2.6449504	-2.9760246	0.7405303
H	0.5336611	-2.9114992	0.8753239
C	3.7389732	-0.8921522	0.0736395
C	3.8453374	-2.2593717	0.4554685
H	2.7119964	-4.0035669	1.0874495
C	4.9284030	-0.1900403	-0.2276024
C	5.1138068	-2.8708269	0.5568243
C	6.1621716	-0.8212016	-0.1299339
H	4.9123997	0.8389439	-0.5580396
C	6.2686136	-2.1645371	0.2697625
H	5.1605804	-3.9126983	0.8623662
H	7.0572106	-0.2563015	-0.3743907
H	7.2416077	-2.6402076	0.3450746
H	0.0091347	0.6910981	0.1953925
N	2.4722284	-0.2916886	-0.0102554
C	2.3997855	1.1375439	-0.4079671
H	1.5607591	1.6028626	0.1026949
H	3.2820745	1.6365554	-0.0123057
C	-2.3991135	0.9051829	0.8292082
H	-1.5931881	1.4976933	0.4036056
H	-3.3127972	1.4146491	0.5295580
B	-0.2377252	4.6286034	-0.0975631
F	-1.0071827	4.4785603	-1.2728389
F	1.0132056	5.2007486	-0.4189658
F	-0.0335843	3.3563392	0.4951793
F	-0.9211122	5.4636902	0.8140279
C	-2.2746284	0.8281782	2.3518247
H	-2.2863869	1.8419322	2.7661923
H	-3.1042497	0.2665810	2.7939088
H	-1.3359868	0.3484179	2.6469913
C	2.2845464	1.3181489	-1.9225079
H	3.1479452	0.8919719	-2.4440389
H	1.3775479	0.8410300	-2.3072936
H	2.2350576	2.3870724	-2.1556130

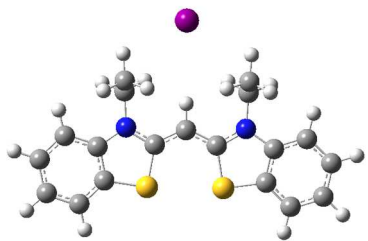
PIC⁺ ClO₄⁻: HF = -1760.61987183 a.u.



Symbol	X	Y	Z
C	-6.0739510	-2.6139896	-0.4662886
C	-4.8837522	-3.1729181	-0.8974262
C	-3.6516217	-2.5235177	-0.6663001
C	-3.6208237	-1.2656450	-0.0004821
C	-4.8451261	-0.7157703	0.4437593
C	-6.0412619	-1.3834433	0.2123088
H	-2.4257770	-4.0216344	-1.6556632
H	-7.0185047	-3.1193775	-0.6425252
H	-4.8744777	-4.1263618	-1.4190046
C	-2.4147696	-3.0902390	-1.0962842
H	-4.8837269	0.2174487	0.9878538
H	-6.9647157	-0.9382838	0.5715391
C	-1.1837108	-1.2070893	-0.1342485
C	-1.2390447	-2.4630191	-0.8322159
H	-0.3123185	-2.8727338	-1.2110992
C	0.0459720	-0.5450004	0.0971029
N	-2.3901319	-0.6233802	0.2122721
C	1.3142709	-1.1660187	0.1882258
C	1.4497813	-2.5414001	0.5864146
C	2.6629203	-3.1381207	0.7180678
H	0.5511199	-3.0830885	0.8496678
C	3.7504161	-1.0427388	0.0763593
C	3.8612860	-2.4134835	0.4439362
H	2.7332623	-4.1695205	1.0526942
C	4.9377246	-0.3329787	-0.2149789
C	5.1318531	-3.0209623	0.5417119
C	6.1738283	-0.9603033	-0.1212153
H	4.9184201	0.6993622	-0.5345911
C	6.2846391	-2.3072201	0.2647020
H	5.1821211	-4.0657888	0.8364455
H	7.0671652	-0.3893288	-0.3576835
H	7.2592887	-2.7799228	0.3373183
H	0.0127294	0.5255423	0.2137896
N	2.4814958	-0.4461689	-0.0036444
C	2.4039917	0.9852201	-0.3916216
H	1.5619976	1.4446596	0.1199065
H	3.2831404	1.4855613	0.0094187
C	-2.3967626	0.6869522	0.9115132
H	-1.5887448	1.2998995	0.5209657
H	-3.3087173	1.2085407	0.6277184
Cl	-0.2430963	4.4919366	-0.0924801
O	1.0810765	5.1793212	-0.2676503
O	-0.0451367	3.2176342	0.6841386
O	-0.8257350	4.1695998	-1.4389523
O	-1.1815299	5.3922825	0.6595718

C	2.2917391	1.1749370	-1.9053314
H	3.1575778	0.7544372	-2.4274471
H	1.3869575	0.6975349	-2.2950390
H	2.2395498	2.2450234	-2.1322252
C	-2.2831345	0.5402287	2.4297366
H	-2.3022735	1.5336849	2.8904291
H	-3.1131499	-0.0447503	2.8394969
H	-1.3440149	0.0514359	2.7082666

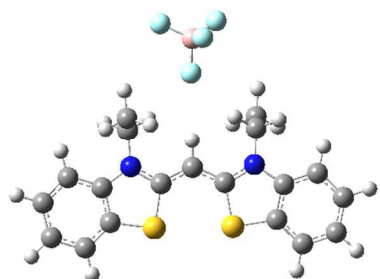
THIA⁺ I: HF = -1652.80626955 a.u.



Symbol	X	Y	Z
C	-5.6165851	-2.9683343	-0.3682013
C	-5.9225821	-1.6472204	-0.0048935
C	-4.9186386	-0.7059748	0.2263850
C	-3.5839186	-1.1088187	0.0852397
C	-3.2867138	-2.4330397	-0.2730266
C	-4.2881844	-3.3758064	-0.5053916
N	-2.4357404	-0.3251806	0.2594553
C	-1.2566039	-0.9912582	0.0829750
S	-1.5468277	-2.6674585	-0.3643654
C	0.0014388	-0.3992727	0.2482115
C	1.2609833	-0.9880554	0.0829958
N	2.4384435	-0.3171311	0.2521650
C	3.5886135	-1.0987545	0.0822856
C	3.2948687	-2.4263768	-0.2659718
S	1.5555118	-2.6666390	-0.3526072
C	4.9222473	-0.6908373	0.2189460
C	5.9287353	-1.6306899	-0.0069051
C	5.6262256	-2.9552702	-0.3603944
C	4.2988831	-3.3677629	-0.4928878
H	-6.4161678	-3.6818845	-0.5422286
H	-6.9602907	-1.3458989	0.1022290
H	-5.1790314	0.3064133	0.5128212
H	-4.0408698	-4.3953304	-0.7837409
H	0.0001487	0.6390762	0.5478412
H	5.1798056	0.3242923	0.4982110
H	6.9656734	-1.3255629	0.0968435
H	6.4277282	-3.6676589	-0.5303114
H	4.0543358	-4.3900349	-0.7634707
C	2.5200935	1.1101998	0.6270363
H	1.6872907	1.6404525	0.1600895
H	3.4259321	1.5060647	0.1637095
C	-2.5198999	1.0975740	0.6508632
H	-1.6937783	1.6366392	0.1820315
H	-3.4315649	1.4949181	0.2006083

I	-0.0113430	4.2400448	-0.6263915
C	2.5403010	1.3200335	2.1423197
H	2.6130856	2.3919698	2.3544726
H	1.6262394	0.9398320	2.6099935
H	3.3985918	0.8198277	2.6025570
C	-2.5269062	1.2896135	2.1686192
H	-2.6000396	2.3588181	2.3941701
H	-3.3800072	0.7820280	2.6304231
H	-1.6079140	0.9057131	2.6234919

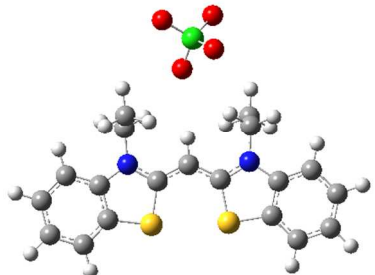
THIA⁺ BF₄⁻: HF = -2065.90894264 a.u.



Symbol	X	Y	Z
C	-5.6791378	-2.7932095	-0.1358110
C	-5.9619651	-1.4185635	-0.1584273
C	-4.9417554	-0.4668309	-0.1595018
C	-3.6144483	-0.9149589	-0.1395196
C	-3.3407516	-2.2907911	-0.1108565
C	-4.3583986	-3.2442066	-0.1106716
N	-2.4527078	-0.1316969	-0.1435850
C	-1.2851640	-0.8387172	-0.0964082
S	-1.6051565	-2.5694773	-0.0756342
C	-0.0155858	-0.2486405	-0.0806170
C	1.2285836	-0.8850401	0.0063292
N	2.4237420	-0.2244532	-0.0154246
C	3.5526124	-1.0487779	0.0811446
C	3.2229172	-2.4074007	0.2011412
S	1.4777591	-2.6188902	0.1773048
C	4.8971548	-0.6550078	0.0691963
C	5.8770819	-1.6412543	0.1860777
C	5.5381696	-2.9976160	0.3103409
C	4.2001587	-3.3952421	0.3182932
H	-6.4910846	-3.5140029	-0.1351935
H	-6.9943820	-1.0823529	-0.1731075
H	-5.1844428	0.5895257	-0.1693573
H	-4.1288712	-4.3047955	-0.0906512
H	0.0073097	0.8303932	-0.1379797
H	5.1837422	0.3853019	-0.0332889
H	6.9223025	-1.3469676	0.1776479
H	6.3197844	-3.7459462	0.3990080
H	3.9270290	-4.4415411	0.4120666
C	2.5518767	1.2337544	-0.2202063
H	1.7039826	1.7273567	0.2535375
H	3.4389815	1.5526364	0.3300522

C	-2.5226444	1.3441602	-0.1087443
H	-1.6549319	1.7454713	-0.6311200
H	-3.3958144	1.6316455	-0.6977467
B	0.1488006	4.8627759	0.1072089
F	1.1462327	5.4866489	-0.6755117
F	0.4848186	4.9694560	1.4755229
F	-1.0964259	5.4886656	-0.1254180
F	0.0605056	3.4937646	-0.2494206
C	-2.6093865	1.8902996	1.3171964
H	-3.4963736	1.5115916	1.8351916
H	-1.7234650	1.6181783	1.8996674
H	-2.6704984	2.9824263	1.2785794
C	2.6519473	1.6069780	-1.7000736
H	3.5199941	1.1352281	-2.1718177
H	1.7522555	1.3057125	-2.2460712
H	2.7578302	2.6927631	-1.7889722

THIA⁺ ClO₄⁻: HF = -2402.16878841 a.u.



Symbol	X	Y	Z
C	-6.0244758	-2.2819510	-0.1383712
C	-6.1495087	-0.8843718	-0.1709382
C	-5.0280491	-0.0544411	-0.1744566
C	-3.7601494	-0.6498525	-0.1465011
C	-3.6442848	-2.0476369	-0.1091475
C	-4.7634353	-2.8797214	-0.1060533
N	-2.5171013	-0.0030858	-0.1509162
C	-1.4371160	-0.8376767	-0.1017272
S	-1.9515216	-2.5206348	-0.0700420
C	-0.1082256	-0.3958237	-0.0945388
C	1.0548813	-1.1696910	0.0004380
N	2.3189803	-0.6542098	-0.0399846
C	3.3441958	-1.6030952	0.0704953
C	2.8591334	-2.9111554	0.2195085
S	1.1011509	-2.9171608	0.2067581
C	4.7252159	-1.3686685	0.0473594
C	5.5844417	-2.4597148	0.1807115
C	5.0906088	-3.7646102	0.3336928
C	3.7154959	-4.0036508	0.3539063
H	-6.9129635	-2.9059337	-0.1360094
H	-7.1370936	-0.4334871	-0.1919598
H	-5.1493686	1.0225331	-0.1920362
H	-4.6557377	-3.9595073	-0.0789852

H	0.0369557	0.6724804	-0.1715618
H	5.1297927	-0.3707559	-0.0757425
H	6.6567046	-2.2893547	0.1635676
H	5.7803467	-4.5968888	0.4354063
H	3.3229518	-5.0089521	0.4704643
C	2.6194291	0.7727866	-0.2805684
H	1.8351245	1.3759367	0.1757876
H	3.5357248	0.9980935	0.2684037
C	-2.4204398	1.4709114	-0.1061979
H	-1.5137332	1.7784501	-0.6260628
H	-3.2555182	1.8597413	-0.6919857
Cl	0.8232929	4.5973648	0.1064567
O	1.4688391	4.0874440	1.3636940
O	-0.3097597	5.5186505	0.4595645
O	1.8383686	5.3428821	-0.7130808
O	0.2959181	3.4343911	-0.6889138
C	-2.4456341	2.0119848	1.3241480
H	-1.5965105	1.6364558	1.9041343
H	-2.3841313	3.1044137	1.2952491
H	-3.3698603	1.7314385	1.8395948
C	2.7708276	1.0927255	-1.7684897
H	3.5741526	0.5033544	-2.2223042
H	1.8423390	0.8937722	-2.3129273
H	3.0132292	2.1537838	-1.8836799

References:

1. Mooi, S. M.; Heyne, B. Size does matter: how to control organization of organic dyes in aqueous environment using specific ion effects. *Langmuir* **2012**, *28*, 16524-16530.
2. Ghasemi, J. B.; Shiri, F.; Deligeorgiev, T. G.; Kubista, M. Thermodynamic characterization of the dimerization equilibrium of newly synthesized polymethine cyanine dyes. *J. Ser. Chem. Soc.* **2008**, *73* (10), 1011-1019.
3. Antonov, L.; Gergov, G.; Petrov, V.; Kubista, M.; Nygren, J. UV-Vis spectroscopic and chemometric study on the aggregation of ionic dyes in water. *Talanta* **1999**, *49* (1), 99-106.

4. Elbergali, A.; Nygren, J.; Kubista, M. An automated procedure to predict the number of components in spectroscopic data. *Anal. Chim. Acta* **1999**, *379* (1-2), 143-158.
5. Kubista, M.; Sjoebäck, R.; Albinsson, B. Determination of equilibrium constants by chemometric analysis of spectroscopic data. *Anal. Chem.* **1993**, *65* (8), 994-998.
6. Kubista, M.; Sjoebäck, R.; Nygren, J. Quantitative spectral analysis of multicomponent equilibria. *Anal. Chim. Acta* **1995**, *302* (1), 121-125.
7. Nygren, J.; Andrade, J. M.; Kubista, M. Characterization of a single sample by combining thermodynamic and spectroscopic information in spectral analysis. *Anal. Chem.* **1996**, *68* (10), 1706-1710.
8. Scarminio, I.; Kubista, M. Analysis of correlated spectral data. *Anal. Chem.* **1993**, *65* (4), 409-16.
9. Physical Constants of water. In *CRC Handbook of Chemistry and Physics. Ed 69th*, Weast, R. C., Ed.; CRC Press: Boca Raton, Florida, **1988-1989**.
10. Didraga, C.; Pugzlys, A.; Hania, P. R.; von Berlepsch, H.; Duppen, K.; Knoester, J. Structure, spectroscopy, and microscopic model of tubular carbocyanine dye aggregates. *J. Phys. Chem. B* **2004**, *108*, 14975-14985.
11. Gulen, D.; Ozcelik, S. Absorption spectrum of monomeric pseudoisocyanine: A new perspective and its implications for formation and spectral response of J-aggregates in solution and in thin films. *J. Lumin.* **2008**, *128* (5-6), 834-837.
12. Ghosh, J. K.; Mandal, A. K.; Pal, M. K. Energy transfer from thiacyanine to acridine orange facilitated by DNA. *Spectrochim. Acta A* **1999**, *55*, 1877-1886.

13. Mandal, A. K.; Pal, M. K. Spectral analysis of complexes of the dye, 3,3 '-diethyl thiacyanine and the anionic surfactant, SDS by the principal component analysis method. *Spectrochim. Acta A* **1999**, *55* (7-8), 1347-1358.

14. Harada, T.; Kurihara, M.; Kuroda, R.; Moriyama, H. On-off switching of the novel thermochromic chiroptical behavior of pseudoisocyanine drive by association/dissociation. *Chem. Lett.* **2013**, *41*, 1442-1444.

15. Norden, B. Linear and circular dichroism of polymeric pseudoisocyanine. *The J. Phys. Chem.* **1977**, *81* (2), 151-159.

16. Streng, W. H. *Characterization of compounds in solution. Theory and Practice*; Kluwer Academic / Plenum Publishers: New York, **2001**.

17. Frisch, M. J.; Trucks, G. W.; Schlegel, H. B.; Scuseria, G. E.; Robb, M. A.; Cheeseman, J. R.; Scalmani, G.; Barone, V.; Mennucci, B.; Petersson, G. A.; Nakatsuji, H.; Caricato, M.; Li, X.; Hratchian, H. P.; Izmaylov, A. F.; Bloino, J.; Zheng, G.; Sonnenberg, J. L.; Hada, M.; Ehara, M.; Toyota, K.; Fukuda, R.; Hasegawa, J.; Ishida, M.; Nakajima, T.; Honda, Y.; Kitao, O.; Nakai, H.; Vreven, T.; Montgomery, J. A.; Peralta, J. E.; Ogliaro, F.; Bearpark, M.; Heyd, J. J.; Brothers, E.; Kudin, K. N.; Staroverov, V. N.; Kobayashi, R.; Normand, J.; Raghavachari, K.; Rendell, A.; Burant, J. C.; Iyengar, S. S.; Tomasi, J.; Cossi, M.; Rega, N.; Millam, J. M.; Klene, M.; Knox, J. E.; Cross, J. B.; Bakken, V.; Adamo, C.; Jaramillo, J.; Gomperts, R.; Stratmann, R. E.; Yazyev, O.; Austin, A. J.; Cammi, R.; Pomelli, C.; Ochterski, J. W.; Martin, R. L.; Morokuma, K.; Zakrzewski, V. G.; Voth, G. A.; Salvador, P.; Dannenberg, J. J.; Dapprich, S.; Daniels, A. D.; Farkas; Foresman, J. B.; Ortiz, J. V.; Cioslowski, J.; Fox, D. J. Gaussian 09, Revision C.01. Wallingford CT, **2009**.

